The EMBO Journal (2004) 23, 3314–3324 | © 2004 European Molecular Biology Organization | All Rights Reserved 0261-4189/04
www.embojournal.org

THE EMBO JOURNAL

Nucleosomes containing the histone variant H2A.Bbd organize only 118 base pairs of DNA

Yunhe Bao[1], Kasey Konesky[1], Young-Jun Park[1], Simona Rosu[1], Pamela N Dyer[1], Danny Rangasamy[2], David J Tremethick[2], Paul J Laybourn[1] and Karolin Luger[1,*]

[1]Department of Biochemistry and Molecular Biology, Colorado State University, Fort Collins, CO, USA and [2]The John Curtin School of Medical Research, Chromatin and Transcriptional Regulation Group, Australian National University, Canberra, Australia

H2A.Bbd is an unusual histone variant whose sequence is only 48% conserved compared to major H2A. The major sequence differences are in the docking domain that tethers the H2A–H2B dimer to the $(H3–H4)_2$ tetramer; in addition, the C-terminal tail is absent in H2A.Bbd. We assembled nucleosomes in which H2A is replaced by H2A.Bbd (Bbd-NCP), and found that Bbd-NCP had a more relaxed structure in which only 118 ± 2 bp of DNA is protected against digestion with micrococcal nuclease. The absence of fluorescence resonance energy transfer between the ends of the DNA in Bbd-NCP indicates that the distance between the DNA ends is increased significantly. The Bbd docking domain is largely responsible for this behavior, as shown by domain-swap experiments. Bbd-containing nucleosomal arrays repress transcription from a natural promoter, and this repression can be alleviated by transcriptional activators Tax and CREB. The structural properties of Bbd-NCP described here have important implications for the *in vivo* function of this histone variant and are consistent with its proposed role in transcriptionally active chromatin.

The EMBO Journal (2004) **23,** 3314–3324. doi:10.1038/sj.emboj.7600316; Published online 15 July 2004
Subject Categories: chromatin & transcription
Keywords: fluorescence resonance energy transfer; histone variant; nucleosome; transcription

Introduction

The nucleosome core particle (NCP) is the fundamental repeating unit in eukaryotic chromatin. In all, 146 bp of DNA is wrapped in 1.65 tight superhelical turns around a histone octamer of two copies each of the four histone proteins (H2A, H2B, H3 and H4) (Luger *et al*, 1997a). The H2A–H2B dimer is tethered to the $(H3–H4)_2$ tetramer by forming a four-helix bundle between the α2 and α3 helices of H2B and H4. In addition, a spatially distinct interface is formed by the ladle-shaped docking domain of H2A that appears to guide the H3αN helix to bind the last turn of the DNA, and forms a short β-sheet with the C-terminal region of H4 (Luger *et al*, 1997a). The histone octamer is not stable under physiological conditions, indicating that the H2A–H2B dimer and $(H3–H4)_2$ tetramer interaction is stabilized significantly by the interaction with DNA.

The organization of DNA into chromatin is generally repressive for DNA replication, transcription, repair and recombination. Therefore, events that alter chromatin conformation are important regulators of these processes. One mechanism to modify the biochemical make-up of the nucleosome is by incorporation of specialized histone variants into nucleosomes to generate an architecturally and functionally distinct local or global chromatin structure. Several variants of the core histone H2A have been identified, which can substitute for replication-dependent H2A (reviewed in Wolffe and Pruss, 1996; Malik and Henikoff, 2003). The newest addition to this list, H2A.Bbd—first identified in humans (Chadwick and Willard, 2001)—associates with other core histones to form nucleosomes *in vivo*, and its distribution appears to overlap that of acetylated H4. H2A.Bbd is largely excluded from the inactive X chromosome, a characteristic that gave this variant its name (*B*arr *b*ody *d*eficient (Bbd); Chadwick and Willard, 2001). These initial findings raise the possibility that H2A.Bbd is enriched in chromatin associated with transcriptionally active regions of the genome.

H2A.Bbd is only 48% identical to major, replication-dependent H2A, making it the most specialized among all histone variants known to date (Malik and Henikoff, 2003; Figure 1A). None of the residues that are the targets of post-translational modification in major-type H2A (acetylation, phosphorylation and ubiquitination) are present in H2A.Bbd (Strahl and Allis, 2000; Chadwick and Willard, 2001). Based on our knowledge of nucleosome structure, the major hallmarks of H2A.Bbd as compared to major H2A are (1) the presence of a continuous stretch of six arginines and the conspicuous absence of lysines in its N-terminal tail; (2) the absence of a C-terminal tail and the very last segment of the docking domain that is responsible for interactions with H3 in major NCP; (3) major sequence differences in the docking domain of H2A (residues 81–119; Figure 1); (4) the presence of only one lysine in H2A.Bbd compared to 14 in major H2A, resulting in a slightly less basic protein (pI 10.7, compared to a pI of 11.2 for major H2A) and (5) the absence of the 'acidic patch' (Luger *et al*, 1997a) (H2A.1 Glu61 to Lys, Glu91 to Arg, Glu92 to Leu; Figure 1A). These changes, either individually or in combination, may alter the interaction between the H2A.Bbd–H2B dimer and the $(H3–H4)_2$ tetramer and/or the DNA, they could change the potential of H2A.Bbd for post-translational modifications, they may modulate the ability of H2A.Bbd-containing nucleosomes to interact with linker histones, or they could affect the type of higher order structure that can be formed by

*Corresponding author. Department of Biochemistry & Molecular Biology, Colorado State University, Fort Collins, CO 80523-1870, USA. Tel.: +1 970 491 6405; Fax: +1 970 491 04941;
E-mail: kluger@lamar.colostate.edu

Received: 15 December 2003; accepted: 16 June 2004; published online: 15 July 2004

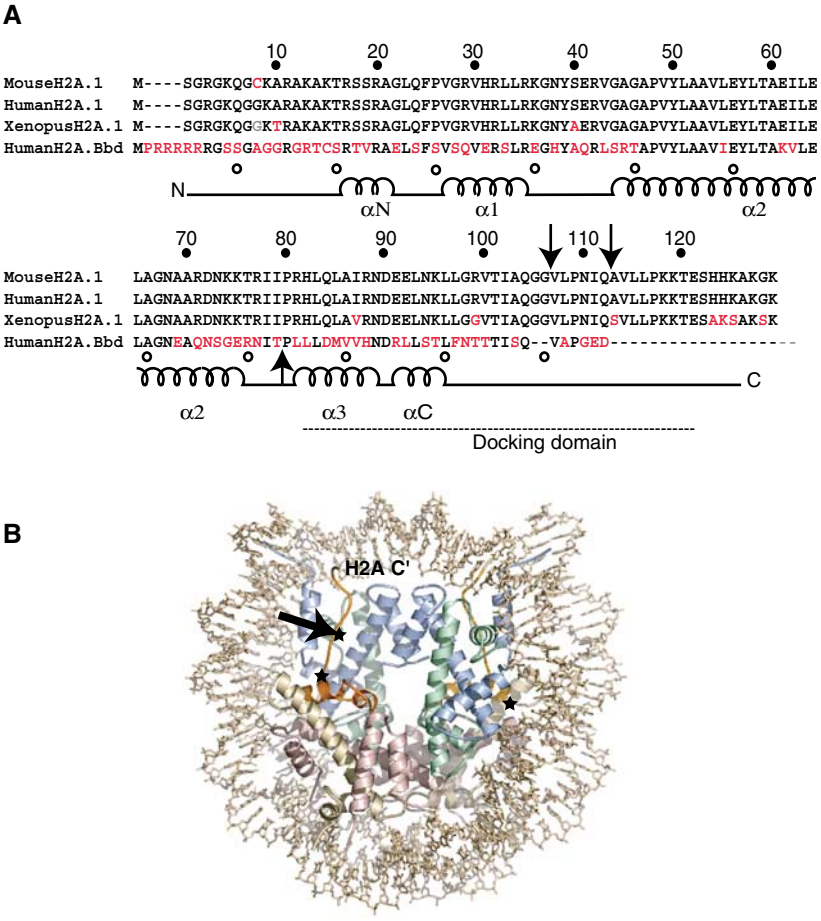

Figure 1 Unique features of H2A.Bbd. (**A**) Sequence alignment of mouse H2A.1 (gi: 121961), human H2A.1 (gi: 106265), human H2A.Bbd (gi: 15553137) and *X. laevis* H2A (gi: 121966). Intervals of 10 amino acids for H2A.1 (filled circles) and H2A.Bbd (open circles) are indicated. Sequence differences are shown in red. The docking domain is indicated by a dashed line. Secondary structure elements of the histone fold (α1, α2 and α3) and extensions (αN and αC) are indicated. Truncated and domain-swapped regions are indicated by arrows. (**B**) Structure of *Xla*-NCP to indicate the structural context of major sequence differences in H2A.Bbd. H2A is shown in yellow, H2B in red, H3 in blue and H4 in green. The H2A docking domain is colored orange and the H2A C-terminus (H2A C) is indicated. The black arrow indicates the approximate C-terminus of H2A.Bbd, based on the sequence alignment shown in (A). Sites of truncation and domain swap are indicated by a star.

these nucleosomes. All of these potential consequences would have significant implications on the biological function of chromatin domains containing this histone variant.

To investigate the effect of H2A.Bbd incorporation on the structure and function of a nucleosome, we analyzed the properties of NCPs in which H2A has been replaced by H2A.Bbd (Bbd-NCP). We show conclusively, using two independent experimental approaches, that Bbd-NCP binds the DNA ends less tightly. To investigate which regions of H2A.Bbd are responsible for this behavior, we analyzed chimeras of H2A in which domains between Bbd and major H2A have been swapped. The ability of Bbd-containing nucleosomes to form regularly spaced arrays on plasmid DNA was also demonstrated. We found that Bbd-containing nucleosomes are spaced more closely, and that this chromatin represses transcription from a natural promoter only slightly less efficiently than chromatin reconstituted with major-type histones. This repression is alleviated upon addition of transcriptional activators Tax and CREB, and appears to be less dependent on the coactivator p300.

Results

H2A.Bbd does not refold to a histone octamer with the other three core histones

The histone variant H2A.Bbd colocalizes with the other three core histones *in vivo*, but to date no *in vitro* analysis of H2A.Bbd-containing nucleosomes exists. To address whether purified recombinant H2A.Bbd can replace histone H2A to form a histone octamer, equimolar amounts of denatured human H2A.Bbd and mouse H2B, H3 and H4 (and, in a control reaction, mouse H2A, H2B, H3 and H4) were refolded by dialysis against a buffer containing 2 M salt. Note that the sequences of H2A.Bbd from mouse and humans are virtually identical (DJ Tremethick, unpublished observations). The refolded histone complexes were purified by size exclusion chromatography. Major-type mouse histones, just as those from *Xenopus laevis*, readily refold to a histone octamer, as demonstrated by a single peak at the appropriate elution volume (Figure 2A) and by the presence of a full complement of all four histones in the peak (Figure 2B). However, replacement of major H2A with H2A.Bbd in the refolding reaction results in two peaks that elute in the position of the

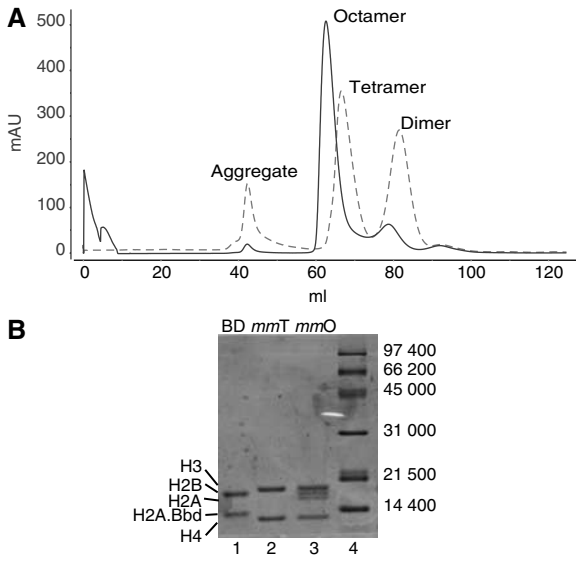

Figure 2 H2A.Bbd does not refold to a histone octamer with H2B, H3 and H4. (**A**) Gel filtration of refolding reactions from mouse histones (octamer, solid line) and mouse H3, H4, H2B and H2A.Bbd (tetramer and dimer, dashed line). (**B**) Fractions containing mouse tetramer (*mm*T, lane 2), H2A.Bbd–H2B dimer (BD, lane 1) and mouse octamer (*mm*O, lane 3) were analyzed by 18% SDS–PAGE, stained with Coomassie brilliant blue.

H2A–H2B dimer and $(H3–H4)_2$ tetramer (Figure 2A; Dyer *et al*, 2004). Analysis of the fractions by SDS–PAGE confirmed that the first tetramer peak contains histones H3 and H4, while the second peak contains H2A.Bbd and H2B (Figure 2B).

Histone octamers are not stable under physiological conditions in the absence of DNA. High ionic strength is required to maintain the protein complex in the absence of the counterbalancing charges provided by the DNA. Nevertheless, crystallographic studies have shown that histone–histone interactions within the histone octamer at high ionic strength are virtually identical to those observed in the NCP at low salt (Luger *et al*, 1997a; Chantalat *et al*, 2003). Thus, our results indicate that the incorporation of H2A.Bbd results in a destabilized interface between the H2A.Bbd–H2B dimer and the $(H3–H4)_2$ tetramer.

H2A.Bbd forms nucleosome core particles with slower electrophoretic mobility

Mouse histone octamer and a 146 bp α-satellite DNA fragment were combined to yield mouse nucleosome core particle (*mus musculus* NCP, or *mm*-NCP) by salt gradient deposition (Dyer *et al*, 2004). Nucleosomes containing *X. laevis* histones were reconstituted similarly, yielding *Xla*-NCPs. Reconstitution from *Xla* octamer and DNA results in a heterogeneous population of NCPs with respect to the position of the DNA on the histone octamer (Dyer *et al*, 2004). A simple heating step (37–55°C for 20–180 min) is usually sufficient to convert this mixture to a uniquely positioned species, which is suitable for biochemical studies and crystallization. Analysis by gel electrophoresis under native conditions shows that *mm*-NCP (Figure 3A, lanes 5 and 6) behaves very similar compared to *Xla*-NCP (Figure 3A, lanes 1 and 2). This is expected, since the four core histones are highly conserved between these two species (H2A: 92.3%, H2B: 92.8%, H3: 95.5%, H4: 100%).

To reconstitute nucleosomes containing H2A.Bbd, H2A.Bbd–H2B dimers, $(H3–H4)_2$ tetramers and α-satellite 146 bp DNA were mixed in a 2:1:1 ratio, and dialyzed as described above. The thus obtained Bbd-NCPs behave quite differently upon analysis by native PAGE (Figure 3A, lanes 3 and 4). Two bands (the upper being much more prominent than the lower) that migrate slower than *Xla*-NCP or *mm*-NCP were consistently obtained, and neither their position nor their relative distribution changes upon heat treatment (Figure 3A, compare lanes 3 and 4). To rule out the possibility that these differences were the result of variations in the assembly method, that is, by using separately purified H2A.Bbd–H2B dimer and $(H3–H4)_2$ tetramers instead of histone octamer during reconstitution, we reconstituted *mm*-NCP from separately refolded H2A–H2B dimer and $(H3–H4)_2$ tetramer. Analysis by native PAGE clearly showed that such nucleosomes were indistinguishable from *mm*-NCP obtained from histone octamer (not shown).

We next determined whether both bands obtained upon reconstitution of Bbd-NCP contained a full complement of histones. We excised the two bands individually and analyzed their content by SDS–PAGE (Figure 3B). The ratio of the four histones in the upper band was determined to be ~1:1:1:1 based on a comparison with a 'mock octamer' (a precise mixture of independently refolded tetramer and Bbd dimer at a 1:2 ratio, compare lanes 4 and 5 of Figure 3B). No depletion of either H2A.Bbd or H2B is evident, as seen in a comparison with lane 3, showing a 1:1 mixture of tetramer and dimer. Unfortunately, the bands are too closely spaced to allow quantification. The lower band of Bbd-NCP was analyzed similarly (Figure 3B, lane 2); however, this species could never be obtained to sufficient amounts to draw a definitive conclusion.

To exclude that the observed results were an artifact of salt-dependent reconstitution (resulting, perhaps, from differences in the affinities of the various histone subcomplexes for DNA at various salt concentrations during the salt gradient), we used yeast Nucleosome Assembly Protein 1 (yNAP-1) to reconstitute nucleosomes under physiological conditions, at 100 mM NaCl. We have shown previously that yNAP-1 has a similar affinity for H2A.Bbd–H2B and (H2A–H2B) dimers (Y-J Park, unpublished observations). For both *mm*-NCP and Bbd-NCP, identical results were obtained upon reconstitution with yNAP-1 and by salt gradient (Figure 3C, compare lane 1 with 3, and 4 with 5), proving that the observed Bbd-NCP species forms independently of the assembly pathway.

Our findings that Bbd-NCP contains stoichiometric amounts of the four histones to form a structurally altered NCP is formally consistent with a non-native particle in which histones are bound to DNA without forming a histone octamer (for example, a 'tetrasome' particle to which two H2A.Bbd–H2B dimers are bound by weak electrostatic interactions. DNase I footprinting is not suited to rule out this possibility, since a 10 bp pattern is not necessarily indicative of an intact NCP (see, for example, Kerrigan and Kadonaga, 1992). We therefore assayed the integrity of Bbd-NCP in the

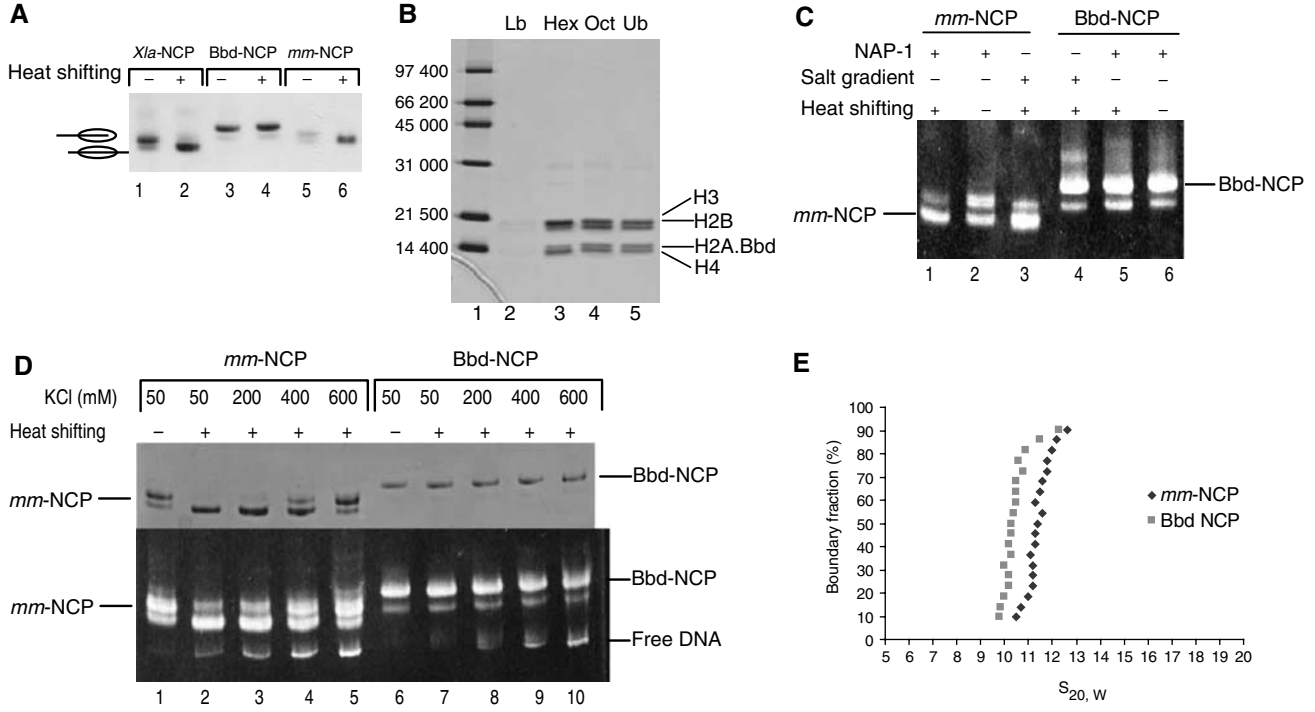

Figure 3 Bbd-NCP is structurally altered. (**A**) Salt gradient reconstituted *Xla*-NCP (lanes 1 and 2), Bbd-NCP (lanes 3 and 4) and *mm*-NCP (lanes 5 and 6), before (−) and after (+) a 1 h incubation at 37°C, were analyzed by 5% native PAGE and stained with Coomassie blue. (**B**) Analysis of the histone content of the two Bbd-NCP nucleosomal bands. The upper band (Ub; lane 5) and lower band (Lb; lane 2) of Bbd-NCP were excised from the native gel and analyzed by 18% SDS–PAGE. H2A.Bbd–H2B dimer: $(H3–H4)_2$ tetramer mixtures of 2:1 (Oct, lane 4) and 1:1 (Hex, lane 3) were used as controls. (**C**) yNAP-1-reconstituted *mm*-NCP (lanes 1 and 2) and Bbd-NCP (lanes 5 and 6) were compared with salt gradient reconstituted NCPs (lanes 3 and 4, respectively) on a 5% native gel, stained with ethidium bromide. (**D**) Stability of *mm*-NCP and Bbd-NCP at elevated ionic strength. Heat-shifted NCPs (lanes 2 and 7) were incubated at 37°C for 1 h in the presence of 200, 400 and 600 mM KCl (lanes 3, 4, 5 and 8, 9, 10). (**E**) The integral distributions of sedimentation coefficients, $G(s)$, obtained for Bbd-NCP and *mm*-NCP after analysis of sedimentation velocity boundaries (van Holde and Weischet, 1978).

presence of increasing ionic strength, under the assumption that non-native charge–charge interactions between histones and the DNA would not be able to withstand elevated ionic strength (Brooks and Jackson, 1994). We incubated the shifted *mm*-NCP and Bbd-NCP in the presence of 200, 400 or 600 mM KCl at 37°C for 1 h (Figure 3D). As demonstrated previously (Muthurajan *et al*, 2003), the translational position of the histone octamer with respect to the DNA changes upon increased ionic strength in NCPs reconstituted with major-type histones (compare, for example, Figure 3D, lanes 2 and 5). Only small amounts of DNA are liberated in the process (Figure 3D, lower panel). Although no redistribution of bands takes place in Bbd-NCP, the complex is stable even at 600 mM salt, and similarly small amounts of DNA are liberated upon incubation at elevated ionic strength. We thus conclude that Bbd-NCP forms a reasonably stable particle that is stabilized by similar interactions as those observed in canonical NCPs.

The altered electrophoretic behavior of Bbd-NCP could be caused by changes in either charge, nucleosome structure, or both. H2A.Bbd is less basic than mouse H2A (with a pI of 10.7 versus 11.2) and has a lower molecular weight, and therefore Bbd-NCP would migrate faster than *mm*-NCP if the two nucleosomes exhibited identical structures. Thus, changes in shape must be responsible for the slow electrophoretic mobility of Bbd-NCP. This was verified by analytical ultracentrifugation. The sedimentation coefficients were 11.6 ± 0.3 for *mm*-NCP and 10.5 ± 0.3 for Bbd-NCP (Figure 3E). This 9.5% difference in S values, which is observed over the entire sedimentation boundary, is significant and reproducible. From the relation $S = M(1-\upsilon\rho)/Nf$, we calculated that the frictional coefficient of Bbd-NCP has increased by 9%. Based on the molecular weight and sedimentation coefficient, we calculate that f/fo (where fo is the frictional coefficient for a sphere) for Bbd-NCP is 1.662 and for *mm*-NCP 1.521, indicating that Bbd-NCP has a more elongated shape than *mm*-NCP.

The DNA ends are less constrained in Bbd-NCP

One simple hypothesis to explain the observed characteristics of Bbd-NCP is that the DNA is less constrained in these particles. Fluorescence resonance energy transfer (FRET) is a powerful tool to determine the distance between two regions within a macromolecular complex. We used this method to test our hypothesis, and to further characterize the structural changes within Bbd-NCP. Nucleosomes exhibit a compact structure at low salt concentration, with the two ends of the DNA at a distance of ~60 Å, but the DNA begins to partially dissociate from the surface of the histone octamer at increased salt concentrations (Park *et al*, 2004). We labeled the two 5′ ends of a 146 bp DNA fragment derived from the 5S rRNA gene (Richmond *et al*, 1988) with fluorescein (FM, acceptor) and coumarin derivatives (CPM, donor), and reconstituted the labeled DNA into *mm*-NCP and Bbd-NCP. We note that the presence of the fluorescent probes does not compromise electrophoretic migration of the samples (data

not shown; Park *et al*, 2004). Samples used for FRET studies were devoid of free DNA, and Bbd-NCP samples usually had a very prominent upper band, and very little of the lower band described above.

Fluorescence was excited at 385 nm, and emission spectra for *mm*-NCP and Bbd-NCP at increasing ionic strength were measured. For *mm*-NCP, we observed a pronounced signal at the acceptor emission wavelength (520 nm) upon excitation of donor emission (Figure 4A). Within *mm*-NCP, FRET between the DNA ends occurs up to a salt concentration of 0.38 M NaCl, but is lost if the ionic strength is further increased, confirming earlier results with *Xla*-NCP (Park *et al*, 2004; Figure 4C). In striking contrast, no FRET is observed in Bbd-NCP even at low ionic strength (Figure 4B), as seen by an absence of fluorescence acceptor emission. Since FRET is concomitant with decreased donor emission, we plotted the ratios between fluorescence emission at 520 and 480 nm for each NCP and for free labeled DNA at several salt concentrations (Figure 4C). In Bbd-NCP, no change in this ratio is observed over the entire salt range measured, as is the case for free DNA. These results were confirmed by monitoring FRET between the DNA ends and the $(H3–H4)_2$ tetramer, with the same results (data not shown). Thus, our results strongly indicate that the ends of DNA in Bbd-NCPs are partially dissociated from the surface of the histone octamer, resulting in a less compact structure. This is a consistent explanation for the observed slower electrophoretic mobility, and the decreased *S* value.

Only 118±2 bp of DNA is protected against micrococcal nuclease digestion in Bbd-NCP

The NCP was originally defined as a stable intermediate from chromatin digestion with micrococcal nuclease (MNase) (Simpson, 1978). Thus, completely folded NCPs reconstituted with 146 bp of DNA should be quite resistant toward digestion, but nucleosomes with only loosely organized DNA ends should be much more susceptible. Mouse octamer (or $(H3–H4)_2$ tetramer and H2A.Bbd–H2B dimers) was reconstituted onto either 146 bp 5S DNA or 196 bp 5S DNA (Georgel *et al*, 1993) to yield nucleosomes (*mm*-146-NCP, Bbd-146-NCP, *mm*-196-NCP and Bbd-196-NCP, respectively). Identical amounts of *mm*-146-NCP and Bbd-146-NCP were incubated with increasing amounts of MNase, and the deproteinized DNA fragments were analyzed on a 10% polyacrylamide gel. A comparison of Figures 5A and B shows that Bbd-146-NCP is digested much more rapidly than *mm*-146-NCP under identical conditions, confirming that the DNA in Bbd-NCPs is relatively less protected from MNase digestion. An intermediate band of ~118 bp is clearly observed at higher MNase concentrations (Figure 5B, lane 6).

To more precisely define the number of base pairs that are actually protected by Bbd-NCPs, we performed a time course of MNase digestion with nucleosomes reconstituted on longer DNA fragments. Figures 5C and D show that digestion of *mm*-196-NCP results in a pronounced stop at ~146 bp, as expected. In contrast, no stop at 146 bp is observed in Bbd-196-NCP, but instead MNase generates a DNA fragment of 118±2 bp in length. Thus, compared to canonical nucleosomes, the terminal ~14 bp of the 146 bp nucleosomal DNA in Bbd-NCP is not protected against digestion, under the assumption that the DNA is symmetrically positioned on the surface of the histone octamer.

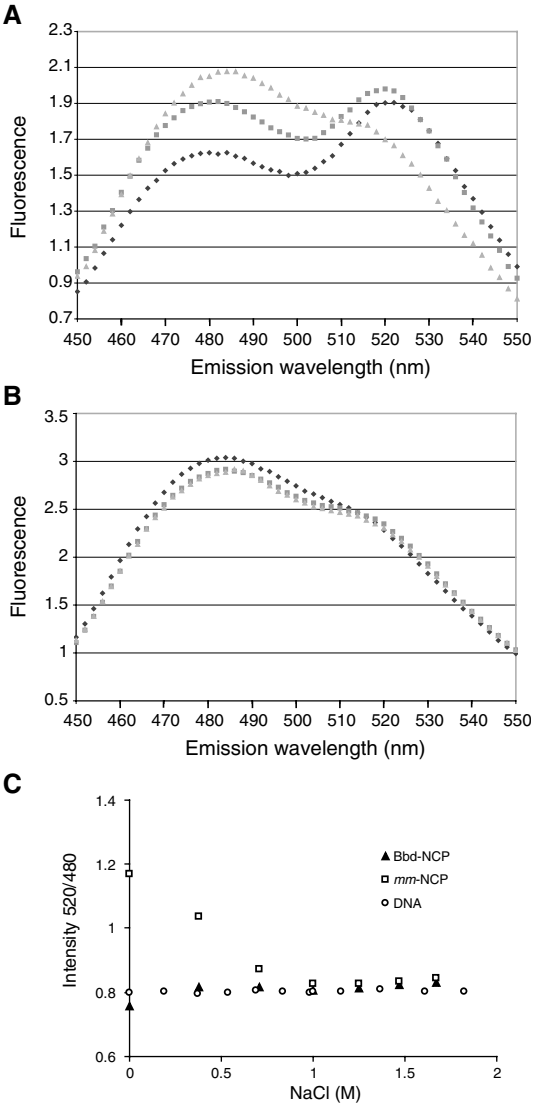

Figure 4 FRET between the two ends of nucleosomal DNA shows that the DNA in Bbd-NCP is less tightly bound. Fluorescence was excited at 385 nm, emission spectra were measured from 450 to 550 nm for *mm*-NCP (**A**) and Bbd-NCP (**B**) at increasing ionic strengths. Only spectra taken at 0, 0.38 and 1 M NaCl are shown (diamonds, squares and triangles, respectively). (**C**) Ratios of fluorescence intensities (520 nm/480 nm) for *mm*-NCP, Bbd-NCP and labeled DNA at the indicated salt concentrations (squares, triangles and circles, respectively) are plotted.

The absence of the C-terminal tail in H2A.Bbd is not responsible for the relaxed structure of Bbd-NCP

One of the obvious differences between H2A and H2A.Bbd is the absence of the basic C-terminal histone tail (which is in a perfect position to organize the terminal regions of the DNA; Figure 1B) in the latter (Figure 1A). C-terminally truncated *Xla* H2A constructs were generated by introducing a stop codon after amino acid 112 (*Xla* $H2A_{112}$, Figure 1). As an additional control, a stop codon was also introduced after amino acid 106, in essence removing the entire 'stem' of the ladle-shaped docking domain (*Xla* $H2A_{106}$, Figure 1). Unexpectedly, both purified truncated histones, together with the three other core histones, could be refolded to

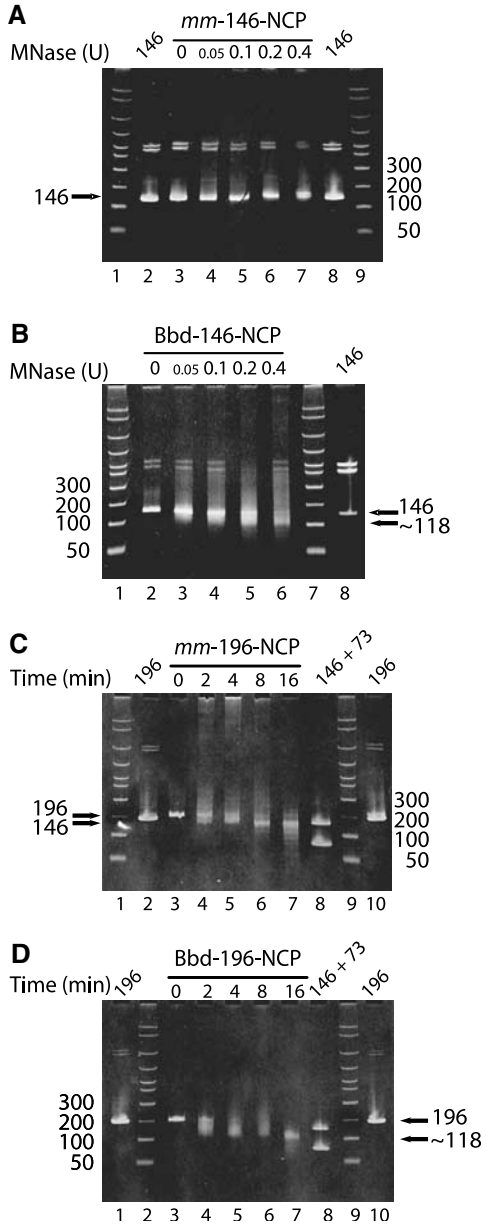

Figure 5 Bbd-NCPs are less resistant against MNase digestion. Identical amounts (2 μg) of *mm*-146-NCP (**A**) and Bbd-146-NCP (**B**) were digested with increasing amounts of MNase (0, 0.05, 0.1, 0.2, 0.4 U) for 1.5 min. Deproteinized samples were analyzed by 10% PAGE, stained with ethidium bromide. For time courses, 10 μg of *mm*-196-NCP (**C**) and Bbd-196-NCP (**D**) was incubated with the same amount of MNase (0.15 U) for the indicated times. In all, 2 μg of sample was removed at 0, 2, 4, 8 and 16 min, and the deproteinized samples were analyzed by 10% PAGE. The 146 bp 5sDNA (146), 196 bp 5sDNA (196) and mixtures of 146 and 73 bp α-satellite DNA (146 + 73) were loaded as controls, as indicated. DNA size markers are given.

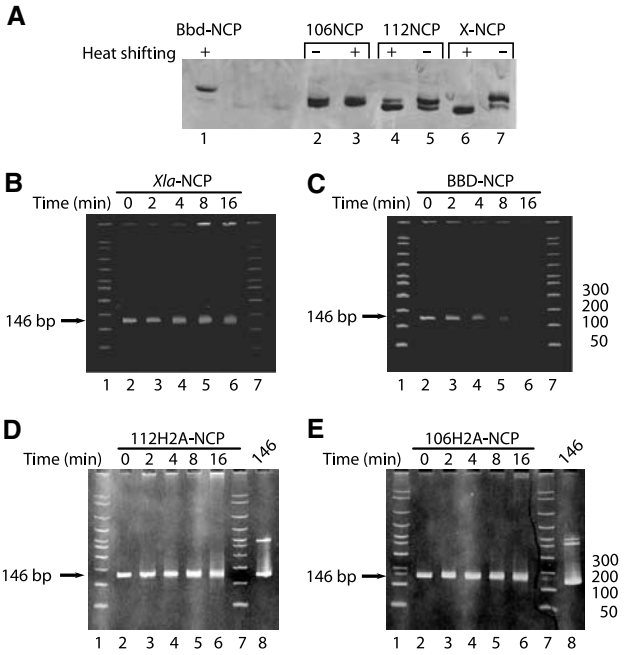

Figure 6 *Xla* $H2A_{106}$-NCP and *Xla* $H2A_{112}$-NCP behave like wild-type *mm*-NCP. (**A**) Salt gradient reconstituted Bbd-NCP (lane 1), *Xla*-NCP (lanes 6 and 7), *Xla* $H2A_{106}$-NCP (106NCP, lanes 2 and 3) and *Xla* $H2A_{112}$-NCP (112NCP, lanes 4 and 5), before (−) and after (+) a 1 h incubation at 37°C, were analyzed by 5% native PAGE, followed by staining with Coomassie blue. (**B–E**) Micrococcal digestion of mutant nucleosomes: 10 μg of *Xla*-NCP (B), Bbd-NCP (C), *Xla* $H2A_{112}$-NCP (D) and *Xla* $H2A_{106}$-NCP (E) were digested with 0.15 U MNase. Aliquots of 2 μg were removed after 0, 2, 4, 8 and 16 min. PAGE (10%) was used to check the deproteinized DNA fragments. 5SDNA (146 bp) (146) was loaded as indicated (D and E, lane 8).

histone octamers using standard procedures (not shown). This indicates that the C-terminal portion of the H2A docking domain and the C-terminal tail are not responsible for stabilizing histone–histone interactions within the histone octamer, despite the presence of several hydrogen bonds between this region and H3 αN and H3 α2 observed in published nucleosome structures (reviewed in Luger, 2003).

We next reconstituted NCPs with these truncated H2A versions. To maintain consistency with Bbd-NCP reconstitutions, $(H3–H4)_2$ tetramer and *Xla* $H2A_{112}$–H2B dimers (or *Xla* $H2A_{106}$–H2B dimers) were reconstituted with 146 bp 5S DNA in a 1:2:1 molar ratio to yield mutant NCPs (*Xla* $H2A_{112}$-NCP and *Xla* $H2A_{106}$-NCP, respectively), using salt gradient deposition. The resulting nucleosomes were analyzed by native PAGE. Figure 6 shows that *Xla* $H2A_{112}$-NCP behaves very similar to *Xla*-NCP. Nucleosomal bands can be shifted almost completely to a band that migrates only slightly slower than *Xla-NCP* (Figure 6A, compare lanes 4 and 5 with lanes 6 and 7). *Xla* $H2A_{106}$-NCP migrates somewhat slower, and can be partly shifted (Figure 6A, lanes 2 and 3). Both truncated nucleosomes are much more similar to full-length *Xla*-NCP and *mm*-NCP in their electrophoretic behavior than to Bbd-NCP. Consistent with this observation, *Xla* $H2A_{106}$-NCPs and *Xla* $H2A_{112}$-NCP exhibit a similar degree of resistance toward digestion with MNase as does *Xla*-NCP (Figures 6B, D and E), and are both much more resistant than Bbd-NCPs (Figure 6C).

Changes in the docking domain are responsible for the altered conformation of Bbd-NCP

Having established that the C-terminal end of the H2A docking domain is not involved in organizing the DNA ends, we turned our attention to the H2A docking domain, where the majority of sequence differences between H2A and H2A.Bbd are clustered. A derivative of *Xla* H2A was prepared in which the original docking domain (from the C-terminal end to I_{79}, Figure 1A) was replaced with the Bbd docking domain (*Xla*

H2A/Bbd). This histone chimera combines two features of interest in H2A.Bbd (the absence of the C-terminal tail and the H2A.Bbd-specific sequence variations in the docking domain), but maintains the sequence of *Xla* H2A in all other regions. Just like H2A.Bbd, this chimeric *Xla* H2A/Bbd histone cannot be refolded to a histone octamer upon combination with the three other histones, but instead forms *Xla* H2A/Bbd–H2B dimers and $(H3–H4)_2$ tetramers (data not shown).

$(H3–H4)_2$ tetramers and *Xla* H2A/Bbd–H2B dimers were reconstituted with 146-mer DNA to form *Xla* H2A/Bbd-NCP, using salt gradient deposition. Analysis of the reconstituted products by gel electrophoresis shows that *Xla* H2A/Bbd-NCP (Figure 7A, lanes 4 and 9) migrates much slower than *Xla*-NCP (Figure 7A, lanes 1 and 2), even somewhat slower than Bbd-NCP (Figure 7A, lanes 7 and 8). Also, just like Bbd-NCP, *Xla* H2A/Bbd-NCP does not reposition upon heat treatment (Figure 7A, compare lanes 4 and 9, and lanes 7 and 8). FRET analysis of *Xla* H2A/Bbd-NCPs confirmed that this is because the ends of the DNA are beyond the critical Förster distance, resulting in the absence of FRET even at low ionic strength, as has been observed in Bbd-NCP. Ratios of fluorescence intensities at 520 and 480 nm are plotted in Figure 7B. Together, the analysis of derivative and chimeric nucleosomes indicates that the region between amino acids 79 and 105 (in *Xla* H2A numbering, Figure 1A) appears to be mainly responsible for either directly or indirectly organizing the ~14 penultimate base pair of nucleosomal DNA.

H2A.Bbd-containing nucleosomal arrays repress transcription from a natural promoter

Having defined the structural changes in H2A.Bbd-containing mononucleosomes, we wanted to investigate whether this histone variant could be efficiently assembled into nucleosomal arrays. H2A.Bbd–H2B dimers and mouse $(H3–H4)_2$ tetramers were assembled onto supercoiled plasmid DNA containing a highly inducible natural promoter (p-306/G-less), using a previously described recombinant assembly system (Georges *et al*, 2002). Recombinant mouse histone octamers and native *Drosophila* histones were assembled as controls. The quality of assembled chromatin and nucleosome spacing was checked by MNase digestion (Figure 8A). H2A.Bbd (together with the other three mouse histones) was assembled into regularly spaced nucleosomal arrays, comparable in quality to the control arrays. However, a Bbd-containing nucleosomal array produces digestion ladders with a repeat length of ~126 bp, whereas nucleosomal arrays reconstituted with either mouse or *Drosophila* histones produce ladders with a repeat length of ~170 bp.

Further, we wanted to know whether such arrays would repress transcription by RNA polymerase II *in vitro* and whether this repression could be alleviated by the action of transcription activators and coactivators, using the well-defined HTLV-LTR *in vitro* system (Georges *et al*, 2002). In this system, nucleosomal arrays efficiently inhibit basal transcription, and this repression is relieved in a Tax/CREB/p300-dependent manner. Bbd-containing nucleosomal arrays inhibit transcription slightly less efficiently than mouse arrays (Figure 8B, compare lanes 3 and 4 with 9 and 10). Tax/CREB-dependent activation is essentially the same (two-fold versus 1.9-fold); however, the effect of p300 was not as pronounced as in mouse nucleosomal arrays (1.3- versus 2.7-fold activation; Figure 8C).

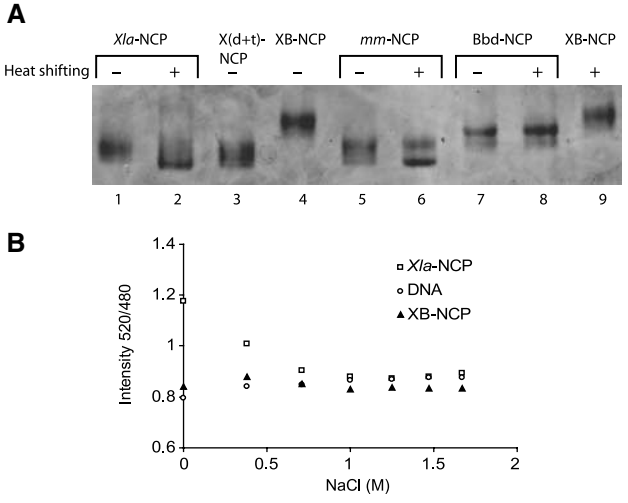

Figure 7 The H2A.Bbd docking domain is responsible for the relaxed structure of Bbd-NCP. (**A**) Salt gradient reconstituted *Xla*-NCP (lanes 1 and 2), *Xla*-NCP reconstituted from H2A–H2B dimer and $(H3–H4)_2$ tetramer (X(d + t)-NCP; lane 3), *Xla* H2A/Bbd-NCP (XB-NCP, lanes 4 and 9), *mm*-NCP (lanes 5 and 6) and Bbd-NCP (lanes 7 and 8), before (−) and after (+) 1 h incubation at 37°C, were analyzed by 5% native PAGE, stained by Coomassie brilliant blue. (**B**) Analysis by FRET. Ratios of fluorescence intensity at 520 and 480 nm for *Xla*-NCP, XB-NCP and labeled DNA at the indicated salt concentrations (squares, triangles and circles, respectively) are plotted. Data points were taken from spectra similar to those shown in Figure 4A and B.

Discussion

The incorporation of histone variants via replication-independent assembly mechanisms has emerged as an important pathway by which eukaryotic cells locally or globally modify chromatin structure to regulate transcription, repair and replication. Histone variants differ from major-type histones in their amino-acid sequence, in their expression patterns and in their pattern of incorporation into chromatin (Malik and Henikoff, 2003; Rangasamy *et al*, 2003). They are as diverse in function as they are in their amino-acid sequence; whereas some are targeted to specialized chromatin regions (for example, the centromeric histone H3 variant; Sullivan, 1998), others, such as H2A.X, serve as markers for chromatin regions where DNA repair is required (d'Adda di Fagagna *et al*, 2003), or play more ill-defined roles in transcription regulation and chromatin higher order structure organization (Perche *et al*, 2000; Chadwick and Willard, 2001, 2002; Fan *et al*, 2002). With the notable exception of H2A.Z (Suto *et al*, 2000; Fan *et al*, 2002), very little biophysical data are available on the effect of any of these histone variants on nucleosome and chromatin structure.

Of all the histone variants, H2A.Bbd is the most specialized in terms of amino-acid sequence, and the least well understood in terms of function. Here we have shown that the interaction between the $(H3–H4)_2$ tetramer and the H2A.Bbd–H2B dimer is weakened compared to that observed between the H2A–H2B dimer and the $(H3–H4)_2$ tetramer. Domain-swap experiments demonstrate that this is due to the sequence differences in the 'base' of the H2A ladle-shaped docking domain. *In vivo*, the weaker interaction between the

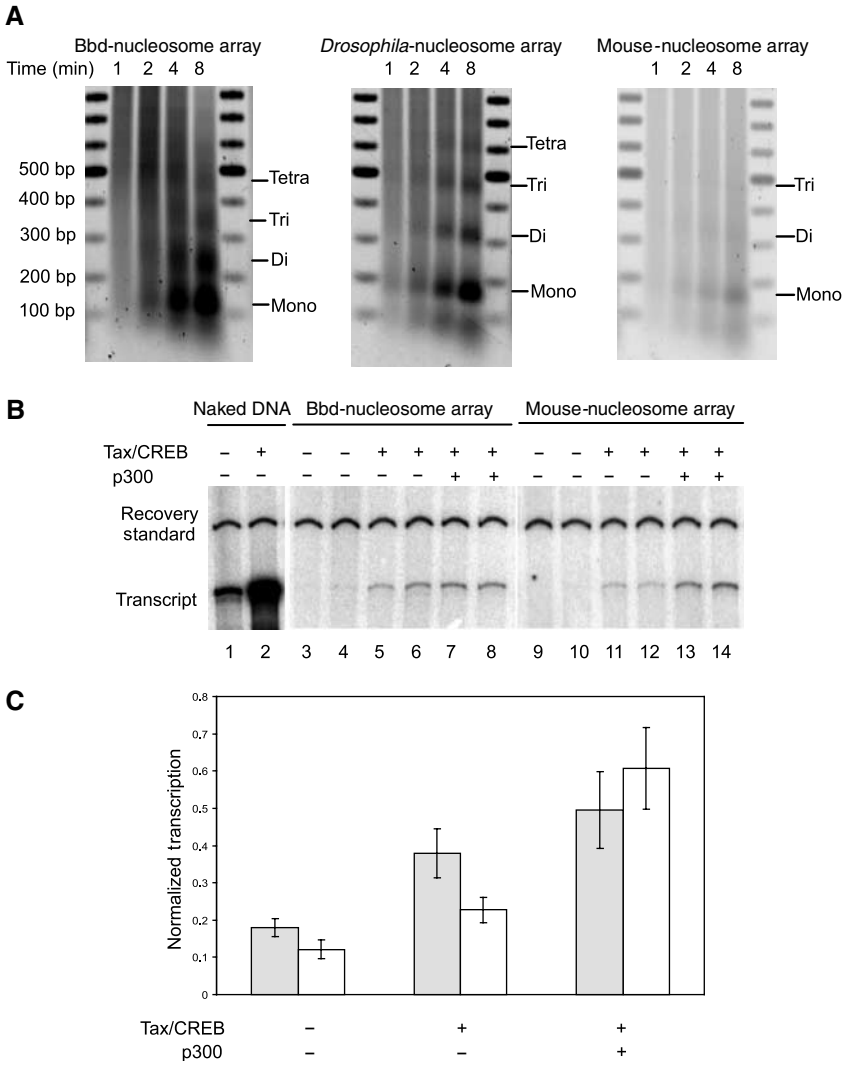

Figure 8 Bbd-containing nucleosomal arrays repress basal transcription. (**A**) In all, 2.1 μg of assembled Bbd-, mouse- and *Drosophila*-nucleosomal arrays was digested with 0.12 U MNase. Aliquots of 0.5 μg were removed after 1, 2, 4 and 8 min, deproteinized and analyzed on 1.2% agarose gels. (**B**) *In vitro* transcription reactions for naked DNA, Bbd-nucleosomal arrays and mouse-nucleosomal arrays are shown. Tax/CREB and p300 were added as indicated above the lanes. Recovery standard and transcript are indicated on the left. (**C**) Results from three transcription assays (from three independent chromatin assembly reactions) were quantified by ImageQuant 5.1 and normalized compared to the recovery standard. Transcripts from mouse and Bbd-nucleosomal arrays are shown by white and gray bars, respectively.

histone subcomplexes within H2A.Bbd nucleosomes may facilitate the dissociation of the H2A.Bbd–H2B dimer from chromatin, either spontaneously or assisted by transcription-related factors such as FACT (Belotserkovskaya *et al*, 2003), histone chaperones (Akey and Luger, 2003) or ATP-dependent chromatin remodeling factors (Becker and Horz, 2002), consistent with its proposed localization in transcriptionally active chromatin (Chadwick and Willard, 2001).

We showed by native PAGE, FRET and MNase digestion that only 118 ± 2 bp of DNA is bound firmly in Bbd-NCP, as opposed to the 147 bp that is tightly organized in canonical NCPs. These results are consistent with a significantly decreased *S* value of the variant particle. Several lines of evidence argue that the observed species is a *bona fide* nucleosome rather than an $(H3–H4)_2$ tetramer–DNA complex with H2A.Bbd–H2B dimers nonspecifically bound. First, Bbd-NCP contains stoichiometric amounts of the four histones. Second, identical complexes are obtained by two independent methods: salt-dependent reconstitution and chaperone-mediated reconstitution under physiological conditions. Third, Bbd-NCP exhibits normal stability in the presence of elevated ionic strength. Finally, we observe that H2A.Bbd-containing nucleosomal arrays exhibit a significantly shorter repeat length (and thus higher nucleosome density). These arrays significantly repress basal transcription, and this repression is relieved in a Tax/CREB-dependent manner.

We demonstrated that the H2A.Bbd docking domain is responsible for the looser DNA organization observed in Bbd-NCP, whereas the missing C-terminal tail plays only a minor role in organizing the 14 penultimate base pairs of nucleosomal DNA. In a structural context, our results suggest that the contact that is made at SHL ± 5.5 (which is organized by the H2A.Bbd–H2B dimer) is still intact, whereas the penultimate contact between the H3 αN helix must be significantly weakened. We interpret these results as evidence that the H2A docking domain (in particular the circular base of the

ladle-shaped substructure) is responsible for orienting the H3 αN helix for proper interactions with the DNA, consistent with the role of this particular region in stabilizing the histone octamer.

To date, this is the first histone variant that forms nucleosomes with such unusual structural properties. H2A.Z, macroH2A or centromeric H3 all form tightly folded nucleosome core particles in our *in vitro* reconstitution system (Suto *et al*, 2000; S Chakravarthy and K Luger, unpublished observations). Dependent on the prevailing histone variant, different physiological outcomes may be obtained since two histone variants may have opposite effects on chromatin structure. For example, whereas H2A.Bbd destabilizes nucleosomal structure, H2A.Z appears to be stabilizing (Park *et al*, 2004); the effect of the incorporation of other histone variants into nucleosomes is not known. The structural properties of Bbd-NCPs described here have important implications for the *in vivo* function of this histone variant. The evidence for the involvement of H2A.Bbd in transcriptionally active chromatin is indirect and mainly stems from the observation that H2A.Bbd colocalizes with acetylated H4 (Chadwick and Willard, 2001). However, consistent with this hypothesis, the observed weakened interaction between the H2A.Bbd–H2B dimer and $(H3–H4)_2$ tetramer, and the less efficient organization of the DNA ends, should present a less formidable obstacle for the advancing RNA polymerase. It is also interesting to speculate that H2A.Bbd-containing nucleosomes may be less dependent on histone modifications and chromatin remodeling. The fact that none of the residues that are the usual targets of post-translational modification in major H2A are present in H2A.Bbd indicates potential consequences for the histone code (Strahl and Allis, 2000) in H2A.Bbd-containing chromatin regions. This hypothesis is supported by our finding that transcriptional activation in Bbd-containing arrays is less dependent on p300 than arrays reconstituted with major-type histones. However, more experiments are needed to investigate the role of H2A.Bbd in particular and of histone variants in general in modulating the transcriptional properties of selected genes.

In summary, we have shown how the replacement of H2A with the histone variant H2A.Bbd alters the conformation of the nucleosome in a way that is consistent with a role in facilitating the transcription process. Clearly, histone variants provide an important alternative way to modulate chromatin structure in addition to, or without the continued need of, histone-modifying enzymes.

Materials and methods

Cloning

The amino-acid sequence of human H2A.Bbd (gi:15553137) was reverse translated into a nucleotide sequence based on an *Escherichia coli* high codon usage table. The gene was synthesized by PCR from four overlapping oligonucleotides spanning the entire sequence (Dillon and Rosen, 1990). The gene was flanked by *Nde*I and *Bam*HI restriction sites. The PCR product was cloned into a PCR-script vector (Stratagene), and the construct was confirmed by sequencing. The H2A.Bbd gene was subcloned into the pET-3a expression vector using the *Nde*I and *Bam*HI cloning sites (Novagen). A stop codon was introduced into the coding region of *Xla* H2A at the codon following amino acid 106 or 112 by site-directed mutagenesis method to obtain truncated *Xla* H2A, *Xla* $H2A_{106}$ and *Xla* $H2A_{112}$. To prepare a domain-swapped derivative of *Xla* H2A, an *Apa*I site (GGGCCC) was introduced into the coding region of *Xla* H2A at $I_{79}P_{80}$ (ATCCCC), resulting in a mutation of I_{79} to G_{79}; an *Apa*I-recognized site was also introduced into the coding region for H2A.Bbd at $T_{83}P_{84}$ (ACTCCG), resulting in a mutation of T_{83} to G_{83}. Plasmids were digested with *Bgl*II and *Apa*I, and the sequence encoding the docking domain of H2A.Bbd was substituted for that of *Xla* H2A. Mouse genes for H2A (P22752), H2B (P10854), H3 (S06755) and H4 (S03426) were cloned using conventional strategies. Mouse H2A and H2B genes were subcloned into pET-3a vectors.

Purification of proteins and DNA

H2A.Bbd was overexpressed in BL21 (DE3) CodonPlus RIL-pLysS cells (Stratagene) for $3\frac{1}{2}$h and lysed by sonication in the presence of 0.2 mg/ml lysozyme and 0.01 mg/ml DNaseI. Standard protocols were used for further purification from inclusion bodies (Dyer *et al*, 2004). Mouse core histones and H2A derivatives (*Xla* $H2A_{106}$, *Xla* $H2A_{112}$, *Xla* H2A/Bbd) were overexpressed in BL21 (DE3)-pLysS (Stratagene) and purified as above. In all, 146 bp DNA was purified as described (Dyer *et al*, 2004). The 196 bp DNA fragment was excised from plasmids containing 12 repeats of a 208 bp DNA fragment (Simpson *et al*, 1985) using *Eco*RI, and the resulting fragment was purified by preparative gel electrophoresis. *Drosophila* NAP-1 (dNAP-1), ISWI and Acf1 were purified as previously described (Ito *et al*, 1996, 1997, 2000; Georges *et al*, 2002); CREB, Tax and p300 were purified as described by Kraus and Kadonaga (1998).

Reconstitution and analysis of nucleosomes

Purified mouse core histones were refolded to histone octamers and purified (Dyer *et al*, 2004). Mouse octamer and purified α-satellite 146 bp DNA (Luger *et al*, 1997a) were reconstituted to NCPs by salt gradient deposition (Dyer *et al*, 2004) to yield mouse-NCPs (*mm*-NCPs). Samples were heated at 37°C for 60 min to shift all nucleosomes to a unique position. For Bbd-NCP, $(H3–H4)_2$ tetramer, H2A.Bbd–H2B dimer and α-satellite 146 bp DNA were mixed in a 1:2:1 molar ratio, and reconstituted using salt gradient deposition to yield Bbd-NCPs. Samples were analyzed on a 5% polyacrylamide gel (Dyer *et al*, 2004). Nucleosomal bands were excised, electro-eluted into 0.05 × TBE buffer, lyophilized and analyzed by 18% SDS–PAGE.

MNase digestion

Histone octamers, or $(H3–H4)_2$ tetramer and H2A.Bbd–H2B dimers were reconstituted with either 146 bp 5S DNA or 196 bp 5S DNA to yield NCPs (*mm*-146-NCP, Bbd-146-NCP, *mm*-196-NCP and Bbd-196-NCP, respectively). Identical amounts of *mm*-146-NCP and Bbd-146-NCP (2 μg NCP per reaction) were digested with increasing amounts of MNase (Worthington) at 37°C in 125 μl of MNase buffer (0.6 mM HEPES (pH 7.6), 52 mM KCl, 5% (vol/vol) glycerol, 1.4% (wt/vol) polyethylene glycol, 5.4 mM $CaCl_2$) for 1.5 min. The reactions were stopped by transferring to tubes containing 12.5 μl TE (10 mM Tris–HCl, 1 mM EDTA, pH 8.0), 12.5 μl 0.5 M EDTA and 200 μl stop buffer (20 mM EDTA, 200 mM NaCl, 1% (wt/vol) SDS, 0.25 mg/ml glycogen). Histones were digested at 37°C for 30 min by adding 20 μl of proteinase K (2.5 mg/ml). For time-course experiments, 0.15 U MNase was used to digest 10 μg NCP of *mm*-196-NCP or Bbd-196-NCP at 37°C in 625 μl MNase buffer. In all, 122 μl aliquots were removed at 0, 2, 4, 8 and 16 min. The reactions were stopped and deproteinized as described above. DNA fragments were extracted, precipitated and analyzed on 10% polyacrylamide gels (in 0.5 × TBE). Gels were scanned, and the center peak for each band was plotted against the log (bp) of the marker to arrive at the actual size of the protected band.

NAP-1-dependent NCP reconstitution

Yeast NAP-1 (yNAP-1) was purified as described (McBryant *et al*, 2003). Mouse octamer, $(H3–H4)_2$ tetramer, H2A–H2B dimer and H2A.Bbd–H2B dimer that had been stored in refolding buffer (2 M NaCl, 10 mM Tris–HCl (pH 7.5), 1 mM EDTA, 5 mM β-mercaptoethanol) were dialyzed against 100 mM NaCl TE buffer (100 mM NaCl, 10 mM Tris–HCl (pH 7.5), 1 mM EDTA). The components were mixed with a 146 bp DNA fragment derived from α-satellite DNA (Luger *et al*, 1997b) in the presence of a two-fold molar excess of yNAP-1 over histone octamer. The reactions were incubated at room temperature for 3 h, followed by a 1 h incubation at 37°C. Assembled NCPs were analyzed by native PAGE.

Analytical ultracentrifugation—Sedimentation volocity assays of nucleosomes were performed using a Beckman XL-A ultracentrifuge

equipped with scanner optics. The initial sample absorbance at 260 nm was about 0.6. Samples in 50 mM KCL TE buffer (50 mM KCL, 10 mM Tris–HC1 (pII 7.5), 1 mM EDTA) were equilibrated in the chamber under vacuum for 40 min at 21°C before sedimentation at 33 000 rpm. Boundaries were analyzed by the method of van Holde and Weischet using Ultrascan data analysis program (version 6.0). Data were plotted as boundary fraction versus $s_{20,w}$ to yield the integral distribution of sedimentation coefficients, $G(s)$. Average sedimentation coefficients were determined from the rate of sedimentation at a boundary fraction equal to 0.5 of the $G(s)$ plot.

Fluorescence resonance energy transfer

The 5′ ends of a 146 bp DNA fragment derived from the 5SrRNA gene (Richmond *et al*, 1988) were derivatized with 7-diethylamino-3-(4′-maleimidylphenyl)-4-methylcoumarin (CPM) and fluorescein-5-maleimide (FM), as described (Park *et al*, 2004). This pair has a Förster distance of 52 Å, the distance at which FRET is 50% efficient. Typically, emission spectra for 0.3 μM of NCP in TE (10 mM Tris–HCL (pH 7.5), 0.1 mM EDTA) were measured using an AVIV spectrofluorometer (Model ATF105). Excitation wavelength was 385 nm. A volume of 5 M NaCl was added to bring the salt concentration from 0 to 0.38, 0.71, 1, 1.25, 1.47 and 1.67 M, respectively, and spectra were taken after a 5 min equilibration period. Ratios of fluorescence intensities were plotted as described.

Reconstitution of nucleosomal arrays

H2A.Bbd–H2B dimers and mouse $(H3–H4)_2$ tetramers were combined in a 2:1 molar ratio and assembled into chromatin using a recombinant assembly system. Core histones were incubated with dNAP-1 (2.4-fold molar excess dNAP-1 over core histones) on ice for 30 min in 25 mM HEPES (K^+ (pH 7.6)), 0.05 mM EDTA and 5% glycerol. ACF (Acf1/ISWI) was added to the core histone/dNAP-1 mix (1:10 molar ratio of ACF to octamer), followed by the addition of an ATP-regenerating system (3 mM ATP, 30 mM phosphocreatine, 1 μg/ml creatine phosphokinase). Supercoiled plasmid DNA (p-306/G-less) was added to assembly reactions and incubated for 4–18 h at 27°C under final conditions of 10 mM HEPES (K^+ (pH 7.6)), 50 mM KCl, 5 mM $MgCl_2$, 5% glycerol, 1% polyethylene glycol and 0.01% NP-40. Assembly reaction volumes were scaled to 150 ng of plasmid DNA in a 7 μl volume (amount added to typical transcription reaction). However, actual reaction volumes ranged from 50 to 200 μl. Supercoiled p-306/G-less contains the HTLV-1 natural promoter sequence (−306 to −1 relative to transcriptional start site) cloned into pUC13, which encompasses the three viral cyclic AMP response elements (vCREs) upstream of the core promoter and a 380-nucleotide G-less cassette (Anderson *et al*, 2000). Mouse octamers were assembled into chromatin using the same system.

MNase digestion was performed on 2.1 μg of assembled DNA (98 μl assembled chromatin). First, chromatin samples were incubated with 135 μl MNase buffer at 37°C for 5 min. Digestion was initiated by addition of 0.12 U MNase at 37°C and 60 μl aliquots were removed after 1, 2, 4 and 8 min of digestion. Nucleic acids were analyzed on a 1.2% agarose gel, followed by SYBR® gold staining and STORM (Molecular Dynamics) imaging. Gene Ruler 100 base pair plus markers (Fermentas) were used as DNA size standards.

In vitro transcription assays

In vitro transcription reactions from assembled chromatin were conducted as previously described (Georges *et al*, 2002), with the following modifications. Preinitiation complexes were formed using 67 fmol of p-306/G-less (150 ng of assembled p-306/G-less in a 7 μl volume) in the presence or absence of exogenous Tax (60 nM), CREB (60 nM) and p300 (6 nM) in a final volume of 30 μl. All reactions contained 50 μM acetyl CoA and 40 μg CEM (HTLV-1 negative T-cell line) nuclear extract. Transcription data were collected using STORM phosphorimaging and quantified by Image Quant 5.1. Transcript levels were normalized to the recovery standard. Fold activation was determined relative to basal transcription (no added activators) for each array.

Acknowledgements

We thank Xu Lu and Jeffrey Hansen for help with analytical ultracentrifugation, and Srinivas Chakravarthy for critical reading of the manuscript. This work was supported by a grant from the Human Frontiers Science Program (HFSPO) to KL and DJT, and by NIH grant # 61909 to KL.

References

Akey CW, Luger K (2003) Histone chaperones and nucleosome assembly. *Curr Opin Struct Biol* **13:** 6–14

Anderson MG, Scoggin KE, Simbulan-Rosenthal CM, Steadman JA (2000) Identification of poly(ADP-ribose) polymerase as a transcriptional coactivator of the human T-cell leukemia virus type 1 Tax protein. *J Virol* **74:** 2169–2177

Becker PB, Horz W (2002) ATP-dependent nucleosome remodeling. *Annu Rev Biochem* **71:** 247–273

Belotserkovskaya R, Oh S, Bondarenko VA, Orphanides G, Studitsky VM, Reinberg D (2003) FACT facilitates transcription-dependent nucleosome alteration. *Science* **301:** 1090–1093

Brooks W, Jackson V (1994) The rapid transfer and selective association of histones H2A and H2B onto negatively coiled DNA at physiological ionic strength. *J Biol Chem* **269:** 18155–18166

Chadwick BP, Willard HF (2001) A novel chromatin protein, distantly related to histone H2A, is largely excluded from the inactive X chromosome. *J Cell Biol* **152:** 375–384

Chadwick BP, Willard HF (2002) Cell cycle-dependent localization of macroH2A in chromatin of the inactive X chromosome. *J Cell Biol* **157:** 1113–1123

Chantalat L, Nicholson JM, Lambert SJ, Reid AJ, Donovan MJ, Reynolds CD, Wood CM, Baldwin JP (2003) Structure of the histone-core octamer in KCl/phosphate crystals at 2.15 A resolution. *Acta Crystallogr D Biol Crystallogr* **59:** 1395–1407

d'Adda di Fagagna F, Reaper PM, Clay-Farrace L, Fiegler H, Carr P, Von Zglinicki T, Saretzki G, Carter NP, Jackson SP (2003) A DNA damage checkpoint response in telomere-initiated senescence. *Nature* **426:** 194–198

Dillon PJ, Rosen CA (1990) A rapid method for the construction of synthetic genes using the polymerase chain reaction. *Biotechniques* **9:** 298–300

Dyer PN, Edayathumangalam RS, White CL, Bao Y, Chakravarthy S, Muthurajan UM, Luger K (2004) Reconstitution of nucleosome core particles from recombinant histones and DNA. *Methods Enzymol* **375:** 23–44

Fan JY, Gordon F, Luger K, Hansen JC, Tremethick DJ (2002) The essential histone variant H2A.Z regulates the equilibrium between different chromatin conformational states. *Nat Struct Biol* **19:** 172–176

Georgel P, Demeler B, Terpening C, Paule MR, van Holde KE (1993) Binding of the RNA polymerase I transcription complex to its promoter can modify positioning of downstream nucleosomes assembled *in vitro*. *J Biol Chem* **268:** 1947–1954

Georges SA, Kraus WL, Luger K, Nyborg JK, Laybourn PJ (2002) p300-Mediated tax transactivation from recombinant chromatin: histone tail deletion mimics coactivator function. *Mol Cell Biol* **22:** 127–137

Ito T, Bulger M, Kobayashi R, Kadonaga JT (1996) *Drosophila* NAP-1 is a core histone chaperone that functions in ATP-facilitated assembly of regularly spaced nucleosomal arrays. *Mol Cell Biol* **16:** 3112–3124

Ito T, Bulger M, Pazin MJ, Kobayashi R, Kadonaga JT (1997) ACF, an ISWI-containing and ATP-utilizing chromatin assembly and remodeling factor. *Cell* **90:** 145–155

Ito T, Ikehara T, Nakagawa T, Kraus WL, Muramatsu M (2000) p300-mediated acetylation facilitates the transfer of histone H2A–H2B dimers from nucleosomes to a histone chaperone. *Genes Dev* **14:** 1899–1907

Kerrigan LA, Kadonaga JT (1992) Periodic binding of individual core histones to DNA: inadvertent purification of the core histone H2B as a putative enhancer-binding factor. *Nucleic Acids Res* **20:** 6673–6680

Kraus WL, Kadonaga JT (1998) p300 and estrogen receptor cooperatively activate transcription via differential enhancement of initiation and reinitiation. *Genes Dev* **12:** 331–342

Luger K (2003) Structure and dynamic behavior of nucleosomes. *Curr Opin Genet Dev* **13:** 127–135

Luger K, Maeder AW, Richmond RK, Sargent DF, Richmond TJ (1997a) X-ray structure of the nucleosome core particle at 2.8 Å resolution. *Nature* **389:** 251–259

Luger K, Rechsteiner TJ, Flaus AJ, Waye MM, Richmond TJ (1997b) Characterization of nucleosome core particles containing histone proteins made in bacteria. *J Mol Biol* **272:** 301–311

Malik HS, Henikoff S (2003) Phylogenomics of the nucleosome. *Nat Struct Biol* **10:** 882–891

McBryant SJ, Park YJ, Abernathy SM, Laybourn PJ, Nyborg JK, Luger K (2003) Preferential binding of the histone (H3–H4)2 tetramer by NAP1 is mediated by the amino-terminal histone tails. *J Biol Chem* **278:** 44574–44583

Muthurajan UM, Bao Y, Forsberg LJ, Edayathumangalam RS, Dyer PN, White CL, Luger K (2003) Crystal structures of histones in mutant nucleosomes reveal altered protein–DNA interactions. *EMBO J* **23:** 260–271

Park YJ, Dyer PN, Tremethick DJ, Luger K (2004) A new FRET approach demonstrates that the histone variant H2AZ stabilizes the histone octamer within the nucleosome. *J Biol Chem*, epub ahead of print

Perche P, Vourc'h C, Konecny L, Souchier C, Robert-Nicoud M, Dimitrov S, Khochbin S (2000) Higher concentrations of histone macroH2A in the Barr body are correlated with higher nucleosome density (in process citation). *Curr Biol* **10:** 1531–1534

Rangasamy D, Berven L, Ridgway P, Tremethick DJ (2003) Pericentric heterochromatin becomes enriched with H2A.Z during early mammalian development. *EMBO J* **22:** 1599–1607

Richmond TJ, Searles MA, Simpson RT (1988) Crystals of a nucleosome core particle containing defined sequence DNA. *J Mol Biol* **199:** 161–170

Simpson RT (1978) Structure of the chromatosome, a chromatin particle containing 160 base pairs of DNA and all the histones. *Biochemistry* **17:** 5524–5531

Simpson RT, Thoma F, Brubaker JM (1985) Chromatin reconstituted from tandemly repeated cloned DNA fragments and core histones: a model system for study of higher order structure. *Cell* **42:** 799–808

Strahl BD, Allis CD (2000) The language of covalent histone modifications. *Nature* **403:** 41–45

Sullivan K (1998) A moveable feast: the centromere/-kinetochore complex in cell division. In *Frontiers in Molecular Biology: Cell Division*, Glover D, Endow S (eds) Oxford: IRL Press

Suto RK, Clarkson MJ, Tremethick DJ, Luger K (2000) Crystal structure of a nucleosome core particle containing the variant histone H2A.Z. *Nat Struct Biol* **7:** 1121–1124

van Holde KE, Weischet WO (1978) Boundary analysis of sedimentation velocity experiments with monodisperse and paucidisperse solutes. *Biopolymers* **17:** 1387–1403

Wolffe AP, Pruss D (1996) Deviant nucleosomes: the functional specialization of chromatin. *Trends Genet* **12:** 58–62

